Distribution Agreement

In presenting this thesis as a partial fulfillment of the requirements for a degree from Emory University, I hereby grant to Emory University and its agents the non-exclusive license to archive, make accessible, and display my thesis in whole or in part in all forms of media, now or hereafter now, including display on the World Wide Web. I understand that I may select some access restrictions as part of the online submission of this thesis. I retain all ownership rights to the copyright of the thesis. I also retain the right to use in future works (such as articles or books) all or part of this thesis.

David Goldberg April 10, 2023

A Jointly Experimental and Theoretical Exploration of *Staphylococcus aureus* Infections and their Control in *Galleria mellonella*

by

David Goldberg

Dr. Bruce Levin

Adviser

Biology

Dr. Bruce Levin

Adviser

Dr. Daniel Weissman

Committee Member

Dr. Nic Vega

Committee Member

2023

A Jointly Experimental and Theoretical Exploration of *Staphylococcus aureus* Infections and their Control in *Galleria mellonella*

By

David Goldberg

Dr. Bruce Levin

Adviser

An abstract of

a thesis submitted to the Faculty of Emory College of Arts and Sciences

of Emory University in partial fulfillment

of the requirements of the degree of

Bachelor of Science with Honors

Biology

2023

Abstract

A Jointly Experimental and Theoretical Exploration of *Staphylococcus aureus* Infections and their Control in *Galleria mellonella*

By David Goldberg

Without the innate and adaptive immune systems, we are nothing more than fleshy flasks to invading bacteria. The innate immune system and all its components clear or reduce the densities bacterial infections to asymptomatic levels. The wax moth, *Galleria mellonella,* has become an attractive model for experimentally exploring the action of innate immune system in the control of bacterial infections. The goal of this investigation is to use mathematical models and computer simulations to generate testable hypotheses about the population dynamics of the control bacterial infection by the innate immune system of *G. mellonella*. Using *Staphylococcus aureus* and *G. mellonella* I estimate the parameters of these models and explore their properties. A particular focus is the contribution of the phagocytes of moth, hemocytes, to the dynamics of infections and the conditions under which they control the infection. The results of this jointly theoretical and experiment study postulate and provide evidence that that phagocytes alone are not sufficient to control. S. aureus infections in *G. mellonella*. Extracellular traps are generated and play the dominant role in controlling these infections.

A Jointly Experimental and Theoretical Exploration of *Staphylococcus aureus* Infections and their Control in *Galleria mellonella*

By

David Goldberg

Dr. Bruce Levin

Adviser

A thesis submitted to the Faculty of Emory College of Arts and Sciences
of Emory University in partial fulfillment
of the requirements of the degree of
Bachelor of Science with Honors

Biology

2023

Acknowledgements

I would like to thank everyone in the EcLF group. In many ways, it's been my home for the past four years. However, with respect to the work inscribed here, I would like to thank a few individuals. I would like to thank Brandon Berryhill, Jason Chen, Josh Manuel, and Teresa Gil for directly contributing to this work. I would like to thank Dr. Eduardo Rodriguez Roman, Andrew Paul Smith, Kylie Burke, Mason Harvill, Jack Peng and Ingrid McCall for their continued friendship and help throughout my time. I would especially like to thank Josh Manuel, Brandon Berryhill and Dr. Eduardo Rodriguez Roman for the comments and feedback during stages of submission. I would like to thank Dr. Vega and Dr. Weissman for providing me with feedback and their work as members of my committee. I would like to thank Tom O'Rourke for his help, support, and friendship during his time. I would like to thank my friends, in particular my roommates, George Poppitz, Eric Zhang, and Josh Kim, for their continued support and their role in my physical, emotional, and professional wellbeing. I would like to thank my parents and my brother for their support in more ways than one can imagine. Finally, I would like to thank Dr. Bruce Levin. None of this work would ever have come to fruition had Bruce not invested so greatly in a random freshman and pushed him to become more.

To the many others who aren't inscribed here as there are more names I wish to list than I have room, thank you. Truly.

Table of Contents

List of Figures and Tables

Figures

Introduction

Thanks to macrophage, neutrophils and other elements of the innate immune system, cutaneous and systemic infections with pathogenic bacteria are either cleared, walled-off in abscesses, or maintained at sufficiently low densities not to manifest symptoms (Suzuki *et al.* 2008; Borregaard 2010). This role of phagocytic leucocytes is well recognized as is their contribution to the course of antibiotic therapy (Sakoulas *et al.* 2017). Nevertheless, with few exceptions (Handel *et al.* 2009; Drusano *et al.* 2011; Ankomah and Levin 2014; Day and Read 2016; Gjini and Brito 2016), little consideration has been given to the negative as well as positive contribution of phagocytic leucocytes to the course of treatments such as antibiotic therapy. The "rational" design of antibiotic therapy is instead based soley on the pharmacokinetics of the antibiotic in the mammalian hosts, and the in vitro pharmacodynamics of the antibiotic and the target bacteria. (Levin and Novachenko 1969; Troup 1991; Craig 1998; Craig 2001; Frimodt-Moller 2002; Toutain *et al.* 2002; Roberts 2011; Sy *et al.* 2016).

Staphylococcus aureus is one such pathogen that represents are large problem for the rational design of antibiotic therapy. Multidrug resistance proliferates within many strains of *S. aureus* (Hiramatsu *et al.* 2014) and at the same time, it encodes many different virulence factors (Ziebandt *et al.* 2004). One such strain, MN8 produces significant quantities of delta-toxin, a hemolysin and important virulence factor which is responsible for permeabilizing membranes (Su *et al.* 2020).

In a relatively recent article, a mathematical model was used to explore the joint action of antibiotics and phagocytic leucocytes in the treatment of acute bacterial infections (Levin *et al.* 2017). With the model employed in that study, depending on the initial bacterial densities and phagocytosis parameters, the infection can be cleared or sustained at pathogen densities lower than in the absence of the phagocytes. However, the conclusions of the model remain to be tested.

Recently, the Greater Wax Moth, *Galleria mellonella,* within the order of *Lepidoptera* has been become increasingly popular as an animal immune model. *Galleria* larvae (worms) are a popular model organism for its low level of consciousness (and therefore its lack of ethical restrictions), its low cost, and its ease of use. Beyond their simplicity, *Galleria* make for an ideal model system for two major reasons: Unlike their mammalian counterparts, *Galleria* lack an adaptive immune system which makes them ideal for testing acute infections and they are excellent systems for evaluating morbidity and mortality due to bacterial infections (Pereira *et al.* 2018).

Despite their popularity, *Galleria* are a relatively poorly understood immune model. There have been some attempts to elucidate the types of hemocytes suspected to be the primary agent in immune function. There are five different categories of hemocytes that have been identified in *Galleria:* prohemocytes, plasmatocytes, granulocytes, spherulocytes, and oenocytes (Pereira *et al.* 2018). However, among those, granulocytes are thought to be the professional immune cell and may also be involved in the production of extracellular defenses included antimicrobial peptides (Pereira *et al.* 2018). Prohemocytes also play an important role

as they are thought to be the progenitor cell for all hemocytes and not differentiated (Senior and Titball 2020).

There has also been some work attempting to culture these cells for primary culture (Senior and Titball 2020). Beyond the hemocytes, it is thought that extracellular traps (ETs) play a role in the innate immune functioning of other *Lepidoptera* and that there may be anti-microbial peptides that circulate to assist in controlling infections. Extracellular traps are named in part for the lymphocyte that produces them but are a general class of extracellular defenses composed of DNA for the control of infections. Extracellular traps cause damage to bacteria and hinder their growth and the best characterized ETs are those produced in neutrophils although they have been found in other species to be produced by other types of immune cells through a general known process ETosis (Papayannopoulos 2018) (Cho and Cho 2019). In other *Lepidoptera*, granulocytes have been found to be the professional cell responsible for cellular immunity responsible for both the dominant amount of phagocytosis and ETs production (Cho and Cho 2019). It was also found that ETs contribute meaningfully to the control of bacterial infections (Cho and Cho 2019). It has been confirmed that *Galleria mellonella* possess the ETs (Chen and Keddie 2021) . However, the exact way these different immune components interact in *Galleria* and which ones are necessary for bacterial infection control is unknown.

Immune system exhaustion may also play an important role in the course of infections. Notably, immune system exhaustion refers to the lack of, or decrease of immune system response or components over the course of an infection. This is most frequently noted in T-cells (Amezquita and Kaech 2017). However, decreased potency and density has also been noted in humans for natural killer cells and macrophages (Mendes *et al.* 2016; Bi and Tian 2017).

Here we use modified and more realistic version of the immune model employed by Levin (Levin *et al.* 2017) using either ET generating leucocytes or phagocytizing leucocytes in the clearance of bacterial infections. The models are similar in that they each demonstrate an ability of the innate immune system to control infections and there is an inoculum density in both models where the infection will become rampant. However, the models differ in that the extracellular traps suggest that there will not be clearance under any conditions and that when infections are controlled, they will reach the same bacterial density independent of inoculum density. The phagocytosis model suggests the opposite in that the level of control after inoculation of bacteria is highly dependent upon initial inoculum density. After modeling and hypotheses were generated, *Staphylococcus aureus* MN8 were injected into worms *in vivo.* The *in vivo* dynamics suggest that the mortality of the worms is highly correlated with the initial inoculum density of the bacteria with only the high density of bacteria able to produce high rates of mortality. The density of the bacteria within the *Galleria* is not significantly different from one another four hours after inoculation with all conditions besides the saline condition being similar in density. Images of the various immune cells isolated are imaged with *Staphylococcus aureus* Newman with a green fluorescent protein, GFP, plasmid to show the functionality of the immune system and its components in action as well as with DAPI to show the presence of the extracellular traps.

Methods

In vivo time inoculations

Galleria (Speedy Worm, wax worms "Crush Proof Bait Puck") were put in the fridge for 24 hours. Afterwards, they were sorted into groups of 10 and placed into petri dishes. These petri dishes were then placed in an incubator at 37ºC overnight. Afterwards, only healthy worms were reselected, and sick or dead worms were removed to avoid confounding errors and groups of 10 were recreated. After groups of 10 were created, inoculated with a 5µL of a low density (1E4), a medium density (1E6), a high density (1E8) of Staphylococcus aureus Newman with NM8 (Dr. Timothy Read bacteria collection) after being washed 4 times with or Dulbecco's PBS (Sigma-Aldrich, D1408). After a period of either 4 or 24 hours elapsed, worms were scored for survival (worms turned dark when sick or completely black and non-moving when dead), morbidity, and Staphylococcus aureus Newman CFUs. To measure CFU by plating on Luria Broth Plates (244510) with a high concentration of streptomycin (Sigma, 081K1275).

Imaging Cells

Galleria (Speedy Worm, wax worms "Crush Proof Bait Puck") were dipped in 100% ethanol (Decon Labs, 2716) and allowed to dry in a sterile petri dish. After drying, worms were picked up by their heads and stabbed in a proleg with a low gage needle (BD, 305195) to bleed the

worm. A p200 was set to 50 µL and sucked up any hemolymph that extrudes from the worms. The hemolymph was then inserted into an Eppendorf tube filled with 1mL of Insect Physiological Saline (IPS; 150mM Sodium Chloride, Fisher, S271; 5mM potassium chloride, Sigma, P-8041; 100mM Tris/HCl, Fisher, BP153; 10mM EDTA, Promega, V4233; 30 mM sodium citrate, J.T. Baker, 3650) kept on ice. Around 20 µL of hemolymph can be expected to be extracted in a given worm although this amount will vary greatly depending on the weight of the worm. After aggregating around 10-15 worms within a single Eppendorf tube, the Eppendorf tube was centrifuged at 500 x g for 10 minutes. The supernatant is pipetted off carefully without disturbing the pellet and the pellet is washed twice with IPS kept on ice and then resuspended in a minimal amount of IPS. Taking extracted cells, Staphylococcus aureus Newman with a GFP-Erythromycin resistance plasmid (Dr. Nic Vega bacteria collection) that was incubated with 20 µg/mL of Erythromycin (Biosynth E-3250) overnight was incubated with hemocytes for 30 minutes in an Eppendorf tube at a high concentration (E6-E8 cfu/mL). After incubation with bacteria, 10 µL of the cells were incubated with 10 µL of 0.4% trypan blue (Sigma, T8154), mounted and imaged on a Leica DMi8 motorized inverted microscope with motorized stage (Leica, 11889113). Additionally, after incubation with bacteria and before trypan blue staining in some cases, the cells were fixed with 4% paraformaldehyde (ThermoFisher, 043368.9M) and stained with 2-(4amidinophenyl)-1H-indole-6- carboxamidine (DAPI, 1 µg/mL; Invitrogen, D1306) or 5 µM DRAQ5 for 10 minutes or and washed with Dulbecco's PBS. Afterwards, 2 drops of antifade mountant (Invitrogen, P36980) and allowing the slide to cure on benchtop for 24 hours. The cells were then imaged on a Nikon A1R HD25 confocal microscope system at 60x oil immersion lens with NA = 1.49.

Results

Two Different *in situ* Models of Immune System Control: Phagocytosis and ETs

Model 1: Phagocytosis Immune System

First, we will present a simplified immune model that is modified from the version employed in TIM (Figure 1). There is a single population of phagocytes. This population of phagocytes is capable of gobbling free bacteria, N_T. Free bacteria when gobbled are labeled as a population N_P and degrade at a rate α when within Leucocytes.

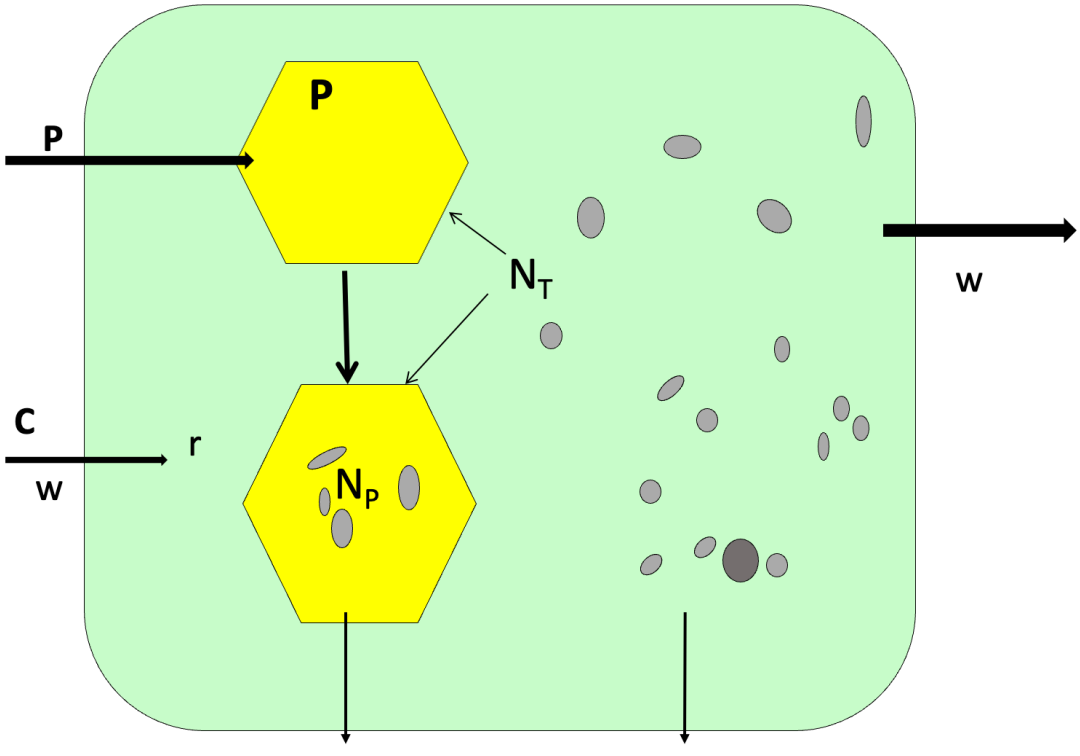

Figure 1. A model of the control of a bacterial infection by phagocytosis. See the text and Table 1 and 2 for definitions and of the variables and parameters and a description of the model.

Free bacteria grow at a rate equal to the product or their maximum growth rate, v (per cell per hour) and the concentration of the limiting resource in the site of the infection, R (μg/ml) as in Monod (1949), $\psi(R) = R/(R+k)$, where k (μg/mL) is the concentration of the limiting resource when the growth rate is half its maximum value, the "Monod constant". Resources are consumed at an equal to product of the density of free bacteria, N, their net growth rate, $v^*\psi(r)$, and a conversion efficiency, e (μg/cell) (Stewart and Levin 1973). The limiting resource enters the site the infection at a rate equal to the rate of flow though the habitat, w (ml per hour) and the concentration in a reservoir, C (μg/ml). We assume that the bacteria within the phagocytes are not replicating.

New phagocytes, P, are recruited and enter the site equal to the maximum number of phagocytes the area can hold multiplied by the flow rate through the habitat w (ml per hour). Phagocytes will also perish at a rate η (per hour) and bacteria within phagocytes will also perish at a rate of α (per hour).

Like Levin (Levin *et al.* 2017), we assume that as the rate of phagocytosis of free bacteria is proportional to the density of free bacteria and phagocytes in site of the infection, but unlike the preceding investigation, we assume that the rate depends on the density of bacteria within the phagocytes and the total density of engulfed phagocytes.

$$\Gamma(N_P, P) = (1 - \frac{N_P}{P * K_{NP}}) * \gamma_{MAX}$$

Where γ_{MAX} is the maximum rate of phagocytosis.

With the variables, parameters, assumptions and functions described above, the rates of change in the concentration of resource, the densities of phagocytes and number of bacteria are given by the below set of coupled differential equations. The definitions of the variables and parameters and values used are separately listed in Table 1 and Table 2.

Variables	Definition	Units	Value
N	Free antibiotic and phage sensitive bacteria	cfu/mL	
P	Free phagocytes	cells/mL	
N_P	Bacteria within Phagocytes	cfu/mL	
R	Resource concentration	μg/mL	

Table 1: Immune Variables

Parameters	Definition	Units	Value
k	Monod constant	μg	1
e	Resource conversion efficiency	μg	5×10^{-7}
C	Reservoir resource concentration	μg/mL	1000
w	Flow Rate	1/h	0.01
γ_{MAX}	Max Phagocyte engulfment parameter	1/h	5×10^{-5}
P_{MAX}	Phagocytes in space	cells/mL	10^6
α	Rate of kill of bacteria with phagocytes	1/h	0.01
η	Rate of loss of phagocytes	cfu/(cell*h)	0.1
K_{NP}	Phagocyte maximum carrying capacity	cfu/cell	20

Table 2: Immune System Parameters

$$EQ1 \quad \frac{d(R)}{dt} = w * (C - R) - e * N * \Psi(R)$$

$$EQ2 \quad \frac{d(N)}{dt} = \Psi(R) * N - w * N - \Gamma(N_P, P) * N * (P) + \eta * N_P$$

$$EQ3 \quad \frac{d(P)}{dt} = P_{MAX} * w - (\eta + w) * P$$

$$EQ4 \quad \frac{d(N_P)}{dt} = \Gamma(N_P, P) * (N) * (P) - N_P * \alpha - w * N_P - \eta * N_P$$

$$\text{where } \Psi(R) = \frac{R}{R+k}$$
$$\Gamma(N_P, P) = (1 - \frac{N_P}{P * K_{NP}}) * \gamma_{MAX}$$

Equation Set 1: Phagocytosis Immune System

Qualitatively, there are three possible outcomes of a bacterial infection for a given immune system: First, the infection remains uncontrolled and the density of the infecting population of bacteria is only limited by availability of nutrients. Second, the infection is controlled, and the density of bacteria is held at a level below that of nutrient limitation. Finally, the infection is cleared by the immune system. The infection will be uncontrolled if rate of phagocytosis is too low to control an infection and the bacterial population will grow to its maximum population, primarily being limited by its access to resources. This will always happen if the inoculum density for an infection is sufficiently large as the cells of the immune system become sufficiently saturated and unable to control the large density of bacteria. A controlled infection will occur if an immune system is too weak to clear it but will prevent the immune system from growing to excess. Notably, an immune system can control an infection at many

different levels and with the parameters below, it will largely depend on the initial inoculum density.

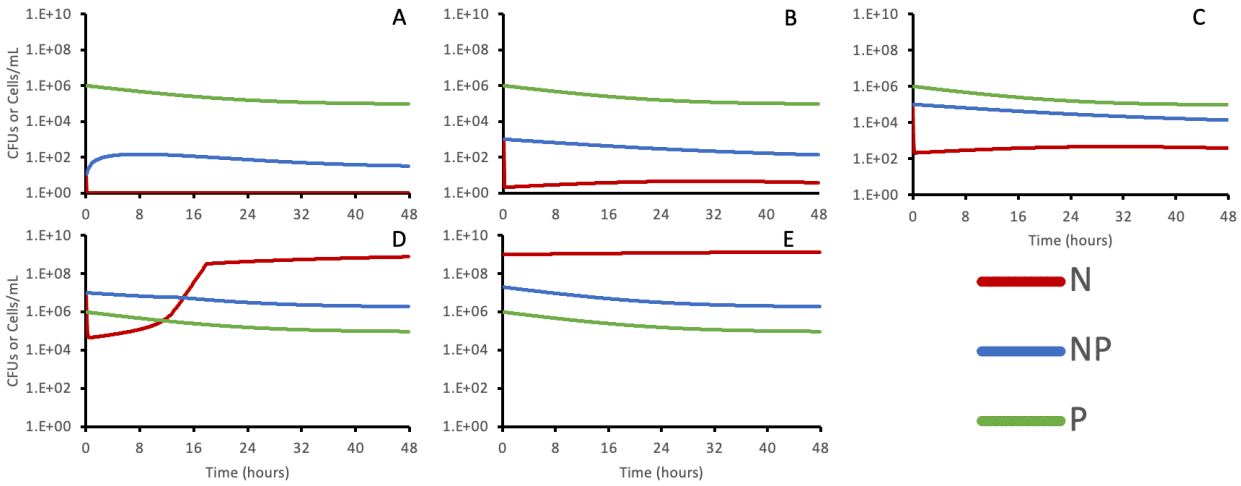

Figure 2: Simulations of the population dynamics for bacterial infections of varying inoculation densities for a phagocytic immune system. Inoculum densities differ by magnitudes of 1E2 where all other variables are held constant with graph A representing E1, B representing E3, C representing E5, D representing E7 and E representing E9.

The infection at a density of E1 is cleared (Figure 2A). The immune system is sufficiently strong and can find and remove the cells before proliferation can ensue. For inoculums E3 and E5 (Figure 2B and C), the infection is controlled at different levels depending on the initial density of the infection. It is notable that both of these densities are low, but they differ by two orders of magnitude. Of particular interest is the inoculum density at E7 (Figure 2D). The bacteria initially appear to be controlled but then eventually result in a rampant infection when the phagocytes become saturated. Also of note is the case seen at the inoculum density of E9 (Figure 2E). When high densities of bacteria are introduced into the lungs of immunocompetent

mice, mortality is observed in nearly all cases after twelve hours (Toews *et al.* 1979) (Onofrio *et al.* 1983) which is what the case of rampant infection after large initial inoculation suggests.

Cleared infections and low density controlled as represented in Figure 2A, 2B and 2C to the point of asymptomatic are the most common type of infection and require no special treatment as they are readily cleared by immunocompetent individuals. Figure 2D and 2E represent the most clinically relevant scenarios as the immune system cannot clear the infection alone and will require help to clear it.

Model 2: Extracellular Trap Immune System

Now, we will consider an immune model similar to the one in Figure 1 in Figure 3. There is a single population of phagocytes. However, now this population of phagocytes instead of gobbling to control the infection, converts itself into Extracellular traps (ETs) to control the bacteria. Free bacteria are trapped within ETs, and while trapped, cannot replicate but do not perish either.

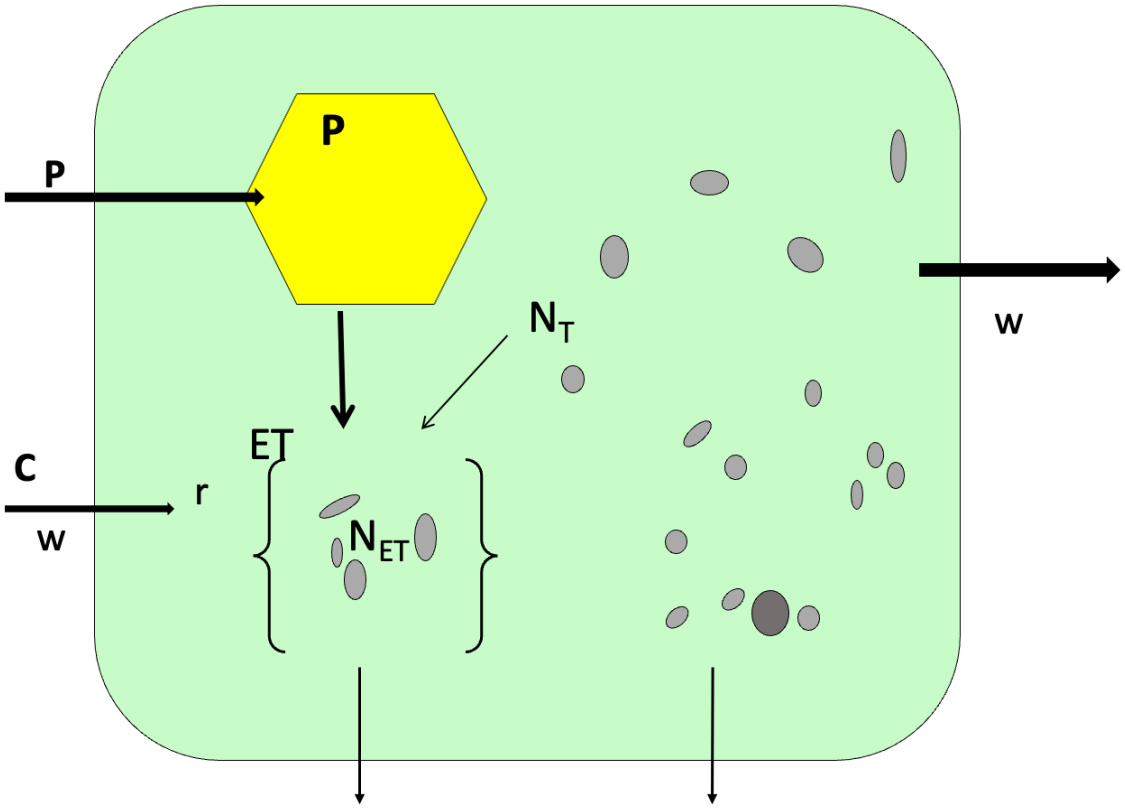

Figure 3. A model of the control of a bacterial infection by ET production. See the text and Table 3 and 4 for definitions and of the variables and parameters and a description of the model.

This model is the same as the first except that the bacteria are not being phagocytized and are not being degraded (α and $\gamma_{MAX} = 0$). Phagocytes will also be destroyed and undergo ETosis to produce ETs at a rate proportional to the density of free bacteria multiplied by a constant θ. ETs will capture bacteria at a rate proportional to the density of free bacteria, N_T, and the density of ETs multiplied by ET_{IN}. Bacteria will escape from ETs at a rate ET_{OUT} which will only depend on the density of bacteria within ETs, N_{ET}. Additionally, ETs will be degraded at a

rate of η_{ET} which will increase depending on the number of bacteria captured within the ETs, N_{ET}.

With the variables and parameters, assumptions and functions described above, the rates of change in the concentration of resource, the densities of phagocytes and number of bacteria are given by the below set of coupled differential equations. The definitions of the variables and parameters and values used are separately listed in Table 3 and Table 4.

Variables	Definition	Units	Value
N	Free antibiotic and phage sensitive bacteria	cfu/mL	
P	Free phagocytes	cells/mL	
ET	Extracellular Traps	ETs/mL	
N_{ET}	Bacteria within ETs	cfu/mL	
R	Resource concentration	μg/mL	

Table 3: Immune Variables

Parameters	Definition	Units	Value
k	Monod constant	μg	1
e	Resource conversion efficiency	μg	5×10^{-7}
C	Reservoir resource concentration	μg/mL	1000
w	Flow Rate	1/h	0.01
θ	ETosis Parameter	ET/(cell*h)	5×10^{-5}
P_{MAX}	Phagocytes in space	cells/mL	10^6
η	Rate of loss of phagocytes	cfu/(cell*h)	0.1
η_{ET}	Rate of loss of ETs	ET/(cell*h)	0.1
ET_{IN}	Capture rate of ETs	1/(ET*h)	10^{-5}
ET_{OUT}	Capture rate of ETs	1/(h)	0.1

Table 4: Immune System Parameters

$$EQ5 \quad \frac{d(R)}{dt} = w * (C - R) - e * N * \Psi(R)$$

$$EQ6 \quad \frac{d(N)}{dt} = \Psi(R) * N - w * N - ET_{IN} * N * ET + ET_{OUT} * N$$

$$EQ7 \quad \frac{d(P)}{dt} = P_{MAX} * w - (\eta + w) * P - N * P * \theta$$

$$EQ8 \quad \frac{d(ET)}{dt} = N * P * \theta - \eta_{ET} * N_{ET} - w * ET$$

$$EQ9 \quad \frac{d(N_{ET})}{dt} = ET_{IN} * N * (ET) - ET_{OUT} * N - w * N_{ET}$$

$$\text{where } \Psi(R) = \frac{R}{R+k}$$

Equation Set 2: Extracellular Trap Immune System

Unlike the phagocytosis model, qualitatively there are only two outcomes when ETs are the mechanism of control: controlled infection and rampant infection. The infection will be uncontrolled if rate of ET control is insufficient to control an infection and the bacterial population will grow to its maximum population, being limited by its access to resource. This will always happen if the inoculum density for an infection is sufficiently large as the ETs of the immune system become degraded and unable to control the large density of bacteria. A controlled infection will occur if an immune system is too weak to clear it but will prevent the immune system from growing to excess. Notably, unlike the phagocytosis model, the inoculum density in a controlled infection will not meaningfully alter the density at which the immune system is controlled.

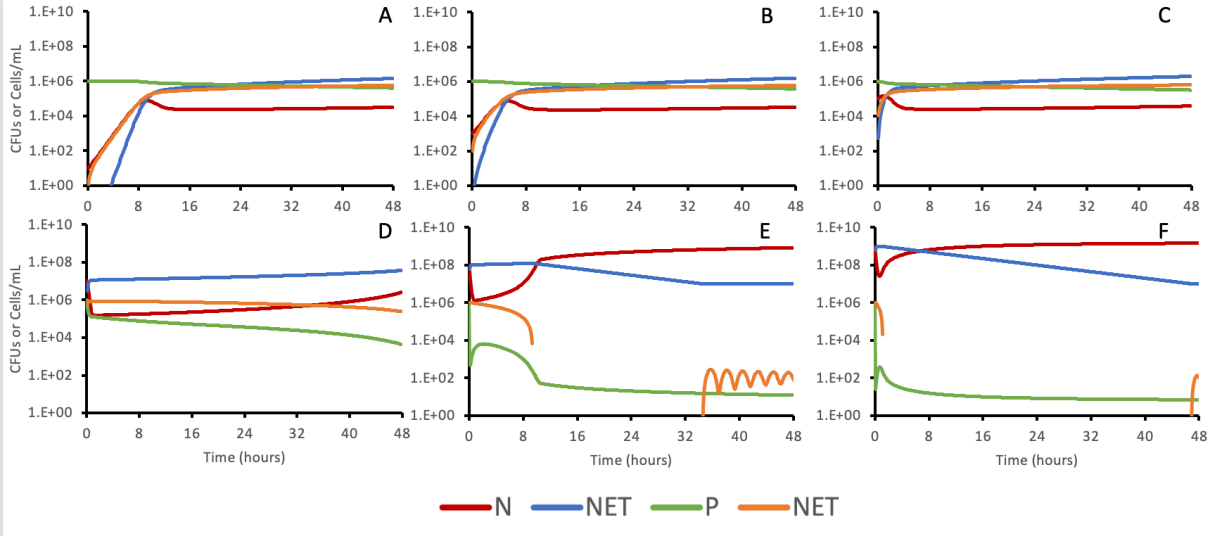

Figure 4: Simulations of the population dynamics for bacterial infections of varying inoculation densities for an extracellular trap immune system. Inoculum densities differ by magnitudes of E1 and E2 where all other variables are held constant with graph A representing E1, B representing E3, C representing E5, D representing E7, E representing E8 and F representing E9.

At no point can this immune system clear infections. The density at E1 (Figure 4A) quickly rises until it looks nearly indistinguishable from the inoculums of E3, E5 and E7(Figures 4B, 4C, and 4D). The difference in bacterial density is less than E1 (Figure 4A). Of particular interest is the inoculum density of E8 (Figure 4E). The bacteria initially appear to be controlled but then eventually result in a rampant infection when the phagocytes are used up and the ETs are degraded. Also, like the phagocytic immune system, when an inoculum density of E9 (Figure F) is introduced, it nearly immediately results in a rampant infection.

Considering the relatively high density of bacteria in the controlled infections, it is unknown whether this would result in an asymptomatic infection from modeling alone. Regardless, it is controlled to a significant degree.

An *In-vivo* Model of the Control of Bacterial Infections Using the Immune System

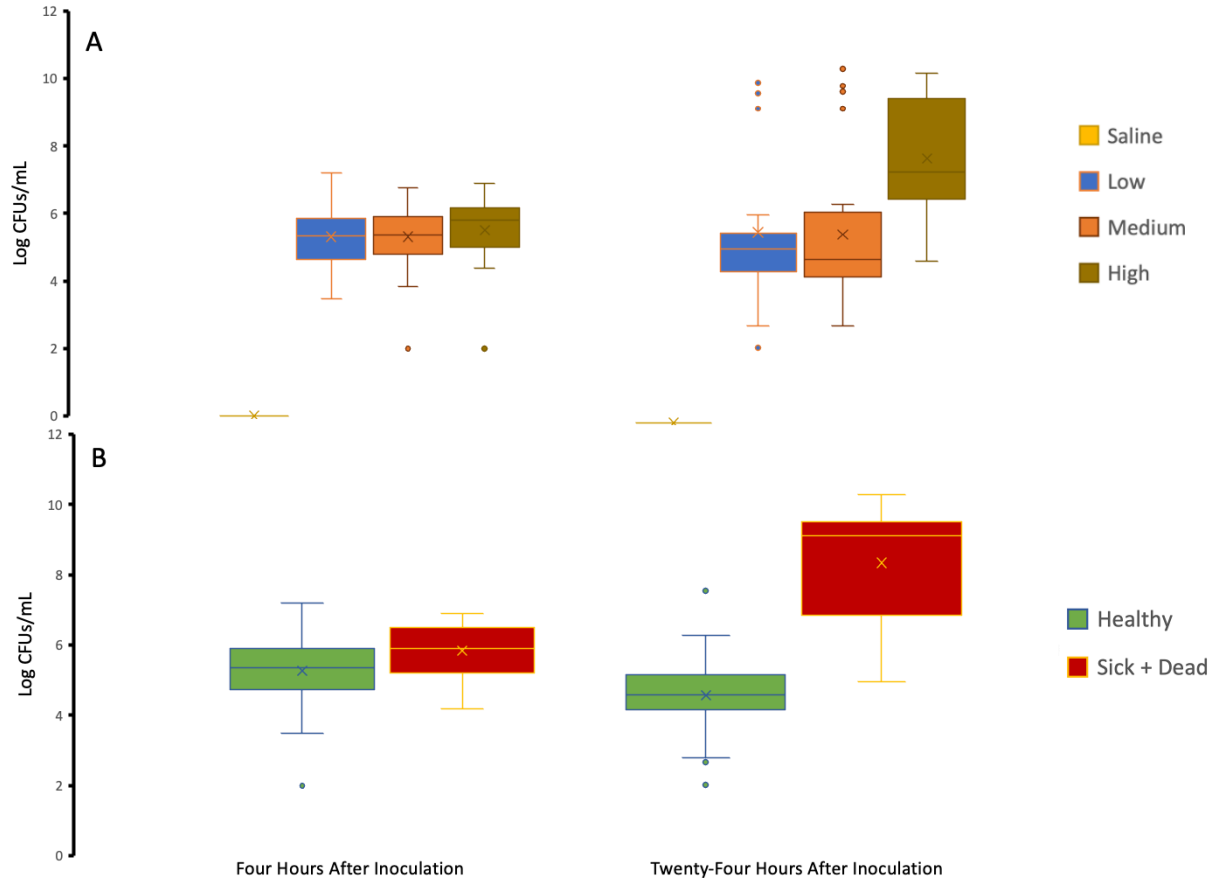

Figure 5: Log CFUs/mL of *in vivo* inoculation of worms with *S. aureus* MN8. Worms were inoculated with varying densities of bacteria, at a low, medium, and high inoculation (differing by E2) and a saline condition which contained no bacteria. At four hours and twenty-

four hours morbidity and mortality were measured. Worms were homogenized in 1mL of saline after four hours and densities were plated on selective plates for the *S. aureus* MN8. Graph A shows the density in log CFUs/mL of the saline, low, medium, and high-density inoculation conditions after four and twenty-four hours. (n=40 for each condition and for each time point). Graph B shows log CFUs/mL for healthy and sick worms at four and twenty-four hours excluding any worms within the saline condition (n=97 healthy four-hour, n=23 sick + dead four-hour, n=73 healthy twenty-four-hour, n=47 sick + dead twenty-four hour).

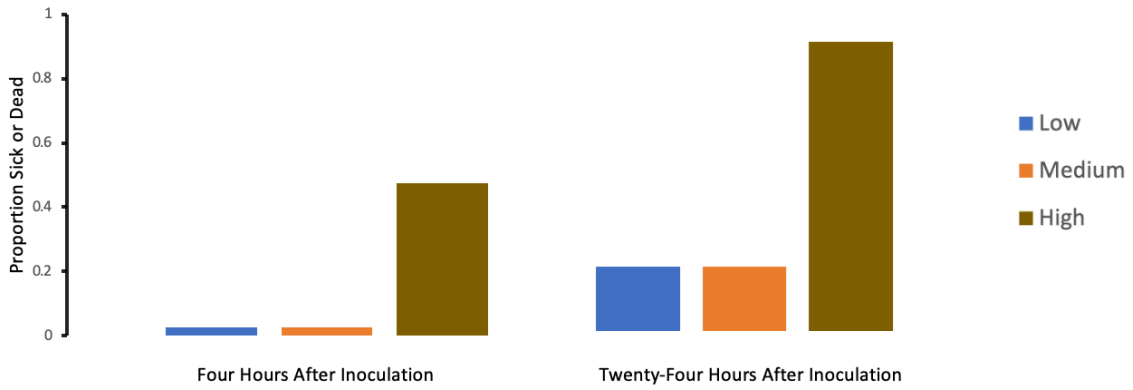

Figure 6: Proportion of worms sick or dead at four hours and twenty-four hours by inoculation condition. Worms were inoculated with varying densities of bacteria, at a low, medium and high inoculation (differing by E2) and a saline condition which contained no bacteria. At four and twenty-four hours, morbidity and mortality were measured (n=40 for each condition at each time point). The saline condition was excluded as there was no mortality in the saline condition at either time point.

An *Ex-vivo* Model of the Control of Bacterial Infections Using the Immune System.

Photos were taken and microscopy was performed to test the integrity of the hemocytes, the presence of phagocytosis and the extracellular traps and whether one was more prolific.

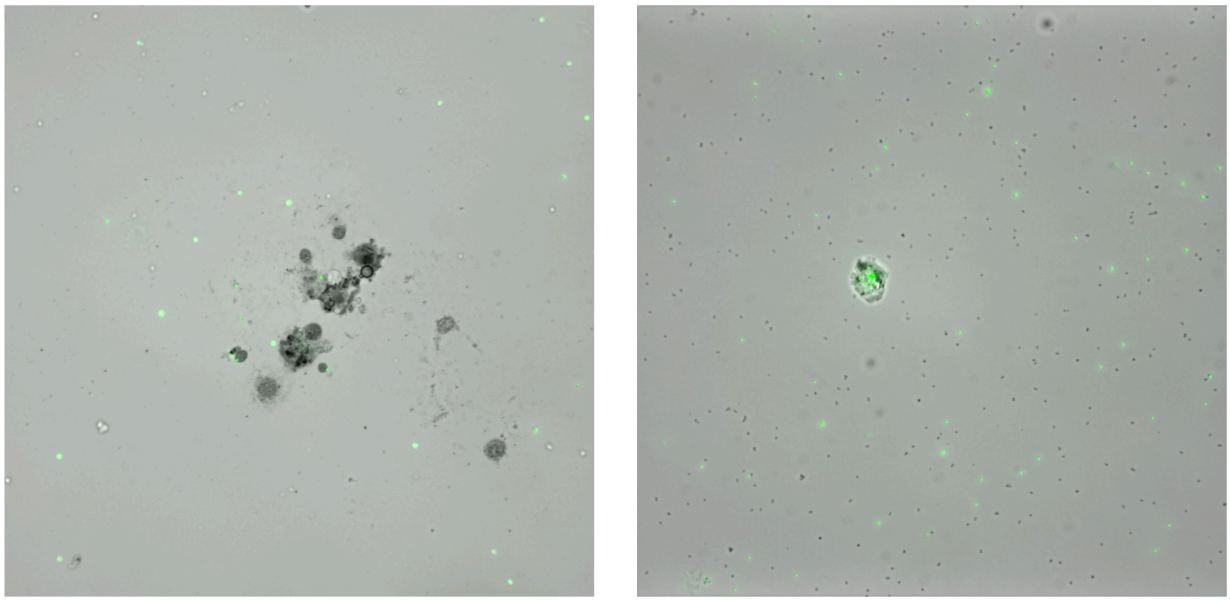

Figure 7: Primary Isolation Hemocytes with GFP *S. aureus*. Hemocytes are first isolated from *Galleria* by stabbing and removing hemolymph and centrifuging and resuspending in saline. Hemocytes were then allowed to incubate for 30 minutes with the GFP *S. aureus.* 10 µL of Hemocytes and *S. aureus* were incubated with 10 µL 0.4% Trypan Blue before being imaged on a Leica DMi8 microscope at 20x magnification.

The small green dots shown in Figure 7 are the *Staphylococcus aureus* with GFP plasmid fluorescing green after excitation. Additionally, the larger white centered shapes with gray outlines are viable hemocytes of various sorts and the ones with dark blackish centers are likely nonviable hemocytes. Figure 7 therefore also shows that viable cells within the hemolymph

exist and can phagocytize bacterial cells. We see an aggregation of multiple GFP bacteria within a single viable hemocyte, likely a granulocyte given its relatively large size and internal membrane composition. This confirms the presence of phagocytosis.

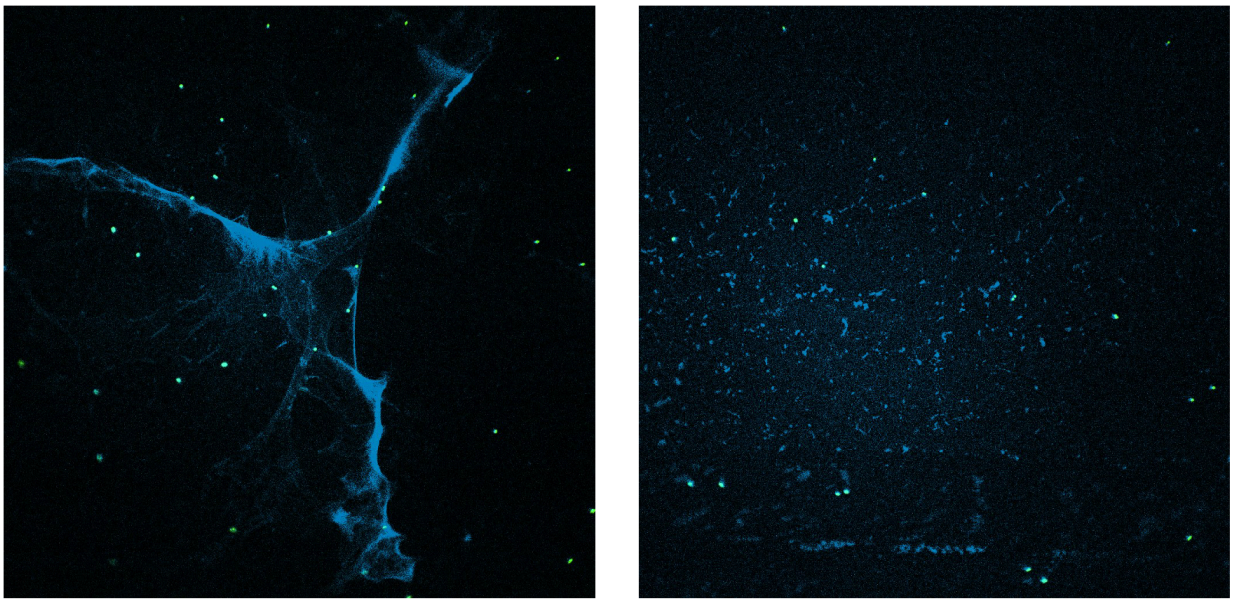

Figure 8: Primary Isolation Hemocytes with GFP *S. aureus* with DAPI. Hemocytes are first isolated from *Galleria* by stabbing and removing hemolymph and centrifuging and resuspending in saline. Hemocytes were then allowed to incubate for 30 minutes with the GFP *S. aureus.* Afterwards cells were fixed and stained with DAPI with (left) and without DNase (right). Images were taken on Nikon A1R HD25 at 60x magnification oil immersion lens.

Similar to Figure 7, in Figure 8 the *Staphylococcus aureus* with GFP plasmid are fluorescing green after excitation. The extracellular traps, composed of DNA, in Figure 8 are stained with DAPI and are fluorescing blue after excitation. The extracellular traps stained with DAPI in Figure 8 are indicative of not only the presence of ETs but its ability to capture bacteria. This picture suggests that the ETs are large and can capture bacteria to a significant extent. We

can see from both images that the extracellular traps are able to aggregate the bacteria and remain attached to them as the presence of ETs results in an increase in relative local bacterial density. Moreover, Figure 8 also demonstrates the ability of DNase to degrade ETs.

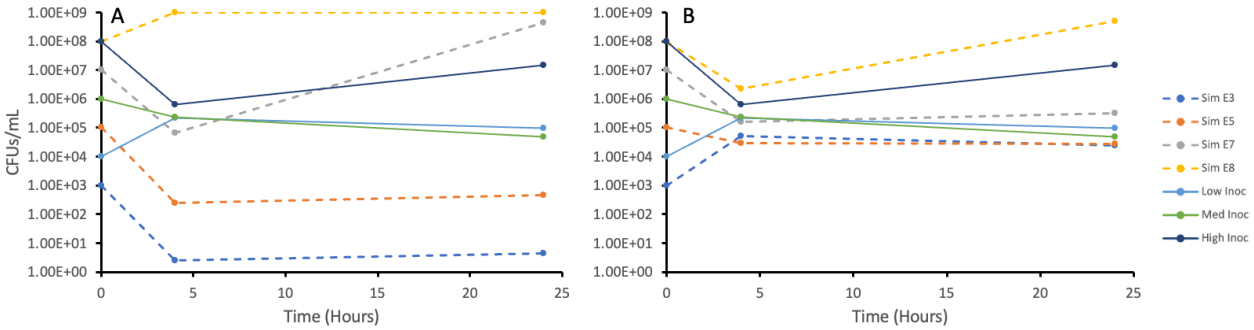

Figure 9: A comparison of the *in vivo* dynamics vs the dynamics simulated by both models. Graph A represents the simulated dynamics at various inoculum densities for the phagocytosis immune system with the dotted lines being the simulated densities and the solid lines being the *in vivo* for the different inoculum densities. Graph B represents the simulated dynamics at various inoculum densities for the ET immune system with the dotted lines being the simulated densities and the solid lines being the *in vivo* for the different inoculum densities. The starting density was estimated for the *in vivo* dynamics.

Discussion

The bacterial inoculation of *G. mellonella in vivo* at the four- and twenty-four-hour time points appears to follow a general trend. Regardless of initial inoculum density, the average and median bacterial densities are all at similar levels irrespective of inoculum density at the four-hour time point and differ from one another by less than E1. At the four-hour time point, the high inoculum is to some degree being controlled and the bacterial density is being lowered, the moderate inoculation experiences a low level of control with their relative density staying relatively unaltered, and the low-density inoculum experience little control and are growing relatively unimpeded. This, at least initially, appears to be far more representative of the ET trap model where bacterial density ended up at the same level after a few hours regardless of inoculum density. If the *in vivo* graphs were more similar to the phagocytosis model, we would expect that the level of persistent infection would be highly dependent upon initial inoculum density. Of note, the worms inoculated with a high density of bacteria suffer far greater rates of illness then their medium or low counterparts which is at least indicative of some effect density dependent effect at the four-hour time point. Yet, despite the worms showing density dependent effect on illness/death, the bacterial density within the sick/dead worms is not significantly different from healthy worms.

At the twenty-four-hour time point, there is a very different story. The low and medium density are virtually indistinguishable from one another. They have identical proportion sick/dead, and median and mean bacterial densities differ from one another by a magnitude less than E1. However, the high-density inoculation is different from the low and medium

density inoculations in terms of median and mean density exceeding it by a magnitude of E3. Moreover, the proportion of sick/dead is at 90%, four and half times greater than either the low or the medium density inoculation. Interestingly as well, the average log CFU/mL is E3 times greater for the sick/dead worms and the average CFU/mL is E4 times greater for the sick/dead worms compared to the healthy worms. The dramatic increase in terms of death and bacterial density for the high inoculation suggests that the inoculation density had a significant effect on the morbidity and mortality for the worms. In truth, both models predict this outcome, however, the nearly unaltered bacterial density from the four-hour time point to the twenty-four-hour time point for the low and medium inoculation conditions is more suggestive of the ET model.

The microscopy also shows the ability of the cells to not only phagocytize cells but also produce ETs. Regarding phagocytosis, this is an infrequent phenomenon. Of the thousands of cells on the slide imaged, only two were noted to have bacteria localized within the membranes of the cells. This could mean that phagocytosis is not the dominant form of control. However, the lack of being able to find these cells is not indicative of lack of control via phagocytosis and is merely indicative of lack of being able to find significant quantities of phagocytosis by hemocytes within this and other samples. Additionally, it should be noted for the ETs, the viability of these bacteria is unknown and their ability to escape is also unknown.

It should also be of note that the evidence of cells phagocytizing bacteria does not preclude the possibility of those same cells later producing extracellular traps for control. It has been thought that phagocytosis of bacteria may be a precondition for ET production. However,

given that the expulsion of DNA and the process of ETosis results in the lysis of the hemocyte, the production of ETs would preclude those same cells also acting as phagocytizing cells.

Given the large quantities of ETs and their relative size and the lack of observable phagocytizing hemocytes, it can be inferred that ETs are the dominant mechanism and may contribute more towards bacterial infection control than phagocytosis. This would certainly support the idea that the extracellular trap model is more important in its contribution to infection control compared to the phagocytosis model. This data corroborates the models and the experiments done *in vivo* and suggests that the mechanism of control may be humoral and facilitated by ETs.

However, this is not a certain conclusion given that no experiments have been performed with ET disruption *in vivo*. Moreover, if extracellular trap disruption occurred, it would still not preclude the possibility of a different humoral response such as antimicrobial peptides from being the dominant method of infection control.

Despite the importance of phagocytosis in many other immune systems, it appears initially that phagocytosis only plays a small role in control. The potential for *Galleria* to be a successful immune model, especially one for exploring the ability of ETs to control bacterial infections, exists. The *in vivo* work exists as a very strong baseline and the *ex vivo* work demonstrates that the hemocytes of *Galleria* can be functional for short periods of time outside of their hosts and can be manipulated to both phagocytize bacteria and produce ETs. Especially the work regarding ETs represents a novel foray in understanding how these systems work in *Lepidoptera* as the work elucidating these mechanisms remains new.

This project and the role extracellular traps play in the control of bacterial infections will be concluded with the following experiments: Repeating the worm experiments *in vivo* but with the inclusion of an additional DNase to disrupt any ET formation and observe the resultant mortality and bacterial densities. Finally, the microscopy experiments can be repeated with DRAQ5, a red nuclear stain that will result in less overlap in emission spectrum with the GFP and will help allow for live cell imaging and observation of ETosis *ex vivo.* Like many things, more work is to always be done, but for an initial exploration, this report will serve as valuable guidelines for those who continue to use *Galleria mellonella* in modeling the control of bacterial infections.

References

Amezquita, R. A., and S. M. Kaech, 2017 The chronicles of T-cell exhaustion. Nature 543: 190-191.

Ankomah, P., and B. R. Levin, 2014 Exploring the collaboration between antibiotics and the immune response in the treatment of acute, self-limiting infections. Proc Natl Acad Sci U S A 111: 8331-8338.

Bi, J., and Z. Tian, 2017 NK Cell Exhaustion. Frontiers in Immunology 8.

Borregaard, N., 2010 Neutrophils, from marrow to microbes. Immunity 33: 657-670.

Chen, R. Y., and B. A. Keddie, 2021 Galleria mellonella (Lepidoptera: Pyralidae) Hemocytes Release Extracellular Traps That Confer Protection Against Bacterial Infection in the Hemocoel. Journal of Insect Science 21.

Cho, Y., and S. Cho, 2019 Hemocyte-hemocyte adhesion by granulocytes is associated with cellular immunity in the cricket, Gryllus bimaculatus. Scientific Reports 9: 18066.

Craig, W. A., 1998 Pharmacokinetic/pharmacodynamic parameters: rationale for antibacterial dosing of mice and men. Clin Infect Dis 26: 1-10; quiz 11-12.

Craig, W. A., 2001 Does the dose matter? Clin Infect Dis 33 Suppl 3: S233-237.

Day, T., and A. F. Read, 2016 Does High-Dose Antimicrobial Chemotherapy Prevent the Evolution of Resistance? PLoS Comput Biol 12: e1004689.

Drusano, G. L., W. Liu, R. Kulawy and A. Louie, 2011 Impact of granulocytes on the antimicrobial effect of tedizolid in a mouse thigh infection model. Antimicrob Agents Chemother 55**:** 5300-5305.

Frimodt-Moller, N., 2002 How predictive is PK/PD for antibacterial agents? Int J Antimicrob Agents 19**:** 333-339.

Gjini, E., and P. H. Brito, 2016 Integrating Antimicrobial Therapy with Host Immunity to Fight Drug-Resistant Infections: Classical vs. Adaptive Treatment. PLoS Comput Biol 12**:** e1004857.

Handel, A., E. Margolis and B. R. Levin, 2009 Exploring the role of the immune response in preventing antibiotic resistance. J Theor Biol 256**:** 655-662.

Hiramatsu, K., Y. Katayama, M. Matsuo, T. Sasaki, Y. Morimoto *et al.*, 2014 Multi-drug-resistant Staphylococcus aureus and future chemotherapy. Journal of Infection and Chemotherapy 20**:** 593-601.

Levin, B. R., F. Baquero, P. P. Ankomah and I. C. McCall, 2017 Phagocytes, Antibiotics, and Self-Limiting Bacterial Infections. Trends Microbiol 25**:** 878-892.

Levin, G. S., and Z. I. Novachenko, 1969 [Hematopoiesis in chronic heliotrine poisoning in Wistar albino rats]. Farmakol Toksikol 32**:** 170-171.

Mendes, F., C. Domingues, P. Rodrigues-Santos, A. M. Abrantes, A. C. Gonçalves *et al.*, 2016 The role of immune system exhaustion on cancer cell escape and anti-tumor immune

induction after irradiation. Biochimica et Biophysica Acta (BBA) - Reviews on Cancer 1865**:** 168-175.

Onofrio, J. M., G. B. Toews, M. F. Lipscomb and A. K. Pierce, 1983 Granulocyte-alveolar-macrophage interaction in the pulmonary clearance of Staphylococcus aureus. Am Rev Respir Dis 127**:** 335-341.

Papayannopoulos, V., 2018 Neutrophil extracellular traps in immunity and disease. Nature Reviews Immunology 18**:** 134-147.

Pereira, T. C., P. P. de Barros, L. R. O. Fugisaki, R. D. Rossoni, F. C. Ribeiro *et al.*, 2018 Recent Advances in the Use of Galleria mellonella Model to Study Immune Responses against Human Pathogens. J Fungi (Basel) 4.

Roberts, J. A., 2011 Using PK/PD to optimize antibiotic dosing for critically ill patients. Curr Pharm Biotechnol 12**:** 2070-2079.

Sakoulas, G., M. Kumaraswamy, A. Kousha and V. Nizet, 2017 Interaction of Antibiotics with Innate Host Defense Factors against Salmonella enterica Serotype Newport. mSphere 2.

Senior, N. J., and R. W. Titball, 2020 Isolation and primary culture of Galleria mellonella hemocytes for infection studies. F1000Res 9**:** 1392.

Su, M., J. T. Lyles, R. A. Petit Iii, J. Peterson, M. Hargita *et al.*, 2020 Genomic analysis of variability in Delta-toxin levels between Staphylococcus aureus strains. PeerJ 8**:** e8717.

Suzuki, T., C. W. Chow and G. P. Downey, 2008 Role of innate immune cells and their products in lung immunopathology. Int J Biochem Cell Biol 40**:** 1348-1361.

Sy, S. K., L. Zhuang and H. Derendorf, 2016 Pharmacokinetics and pharmacodynamics in antibiotic dose optimization. Expert Opin Drug Metab Toxicol 12**:** 93-114.

Toews, G. B., G. N. Gross and A. K. Pierce, 1979 The relationship of inoculum size to lung bacterial clearance and phagocytic cell response in mice. Am Rev Respir Dis 120**:** 559-566.

Toutain, P. L., J. R. del Castillo and A. Bousquet-Melou, 2002 The pharmacokinetic-pharmacodynamic approach to a rational dosage regimen for antibiotics. Res Vet Sci 73**:** 105-114.

Troup, J. D., 1991 Measurement of strength and endurance. The psychophysical lift test. Spine (Phila Pa 1976) 16**:** 679.

Ziebandt, A.-K., D. Becher, K. Ohlsen, J. Hacker, M. Hecker *et al.*, 2004 The influence of agr and σB in growth phase dependent regulation of virulence factors in Staphylococcus aureus. PROTEOMICS 4**:** 3034-3047.